

Photolithographic patterning of subwavelength top emitting colloidal quantum dot based inorganic light emitting diodes on silicon

Ashwini Gopal, Kazunori Hoshino, and Xiaojing Zhang

Citation: *Applied Physics Letters* **96**, 131109 (2010); doi: 10.1063/1.3373832

View online: <http://dx.doi.org/10.1063/1.3373832>

View Table of Contents: <http://scitation.aip.org/content/aip/journal/apl/96/13?ver=pdfcov>

Published by the *AIP Publishing*

Articles you may be interested in

[High color purity ZnSe/ZnS core/shell quantum dot based blue light emitting diodes with an inverted device structure](#)

Appl. Phys. Lett. **103**, 053106 (2013); 10.1063/1.4817086

[Graphene as anode electrode for colloidal quantum dots based light emitting diodes](#)

Appl. Phys. Lett. **103**, 043124 (2013); 10.1063/1.4816745

[Ultraviolet electroluminescence from colloidal ZnO quantum dots in an all-inorganic multilayer light-emitting device](#)

Appl. Phys. Lett. **100**, 061104 (2012); 10.1063/1.3682307

[Efficiency measurement of GaN-based quantum well and light-emitting diode structures grown on silicon substrates](#)

J. Appl. Phys. **109**, 014502 (2011); 10.1063/1.3530602

[Fabrication of genuine single-quantum-dot light-emitting diodes](#)

Appl. Phys. Lett. **88**, 121115 (2006); 10.1063/1.2188057

Frustrated by old technology?

Is your AFM dead and can't be repaired?

Sick of bad customer support?

It is time to upgrade your AFM

Minimum \$20,000 trade-in discount for purchases before August 31st

Asylum Research is today's technology leader in AFM

dropmyoldAFM@oxinst.com

OXFORD
INSTRUMENTS
The Business of Science

Photolithographic patterning of subwavelength top emitting colloidal quantum dot based inorganic light emitting diodes on silicon

Ashwini Gopal, Kazunori Hoshino, and Xiaojing Zhang^{a)}

Department of Biomedical Engineering, University of Texas at Austin, Austin, Texas 78758, USA

(Received 22 January 2010; accepted 3 March 2010; published online 31 March 2010)

The combination of lithographic patterning and nanostamping methods makes it possible to accurately define diffraction-limited multicolor (wavelengths 560–620 nm) light sources on a silicon substrate. We demonstrate a postprocessing technique that utilizes standard photolithography process to pattern the cathode of top emitting diode. Correlation of electroluminescence, photoluminescence, and atomic force microscopy topography showed that the emission region is well defined through the robust multiscale patterning techniques, with the fineness of the emitting area mainly limited by the point spread function of the observing microscope. © 2010 American Institute of Physics. [doi:10.1063/1.3373832]

Site-controlled patterning of light emitting diodes (LEDs) is important in applications such as high resolution arrays,¹ large screen displays,^{2,3} microelectromechanical systems (MEMS),⁴ optoelectronic systems,⁵ and multicolor excitation source in micrototal analysis systems (μ -TAS).⁶ Organic light emitting diodes (OLEDs) have attracted the attention due to its easy integration with displays.^{2,3,7} Conventional photolithographic patterning have been difficult for OLED fabrication due to the failure of the devices on being exposed to water, oxygen, and solvents.^{8–11}

Typical patterning of OLEDs^{12,13} has been demonstrated using shadow-mask technique,^{14,15} laser ablation,¹⁶ and stamping-induced lift off^{17–19} where each has certain shortcomings. Shadow mask techniques have limited resolution¹⁴ because of shadow effects. Cold welding techniques require pressure and temperature control during contact stamping to prevent damage to the organic layers.^{17–19} Alternate methods to pattern OLEDs have been demonstrated by patterning the active layer. Polymer-based LEDs have been patterned utilizing screen printing,²⁰ inkjet printing²¹ soft-lithography,^{22,23} and capillary lithography techniques.²⁴ Resolution in these methods is not comparable with the advanced photolithography.

Photolithography is a commonly used process in fabrication of microelectronic integrated circuits. Such patterning techniques for most advanced devices enable controlled feature size on the order of 100 nm. These have seen wide applications such as complementary metal oxide semiconductor (CMOS) or MEMS. In this paper, we introduce photolithographic patterning of metal cathode for top emitting quantum dot based inorganic light emitting diodes (QD-LED) on silicon substrates. Since our device consists of metals, silicon and metal oxides, standard microfabrication processes can be applied to obtain controlled feature size of the electrode with greater accuracy. We also utilize a nanostamping technique for patterning colloidal QDs. The combination of both methods makes it possible to define multicolor light sources, which open up the possibilities for creating nanophotonic microsystems for imaging and sensing.

The inorganic QD-LED device fabrication starts from a p-silicon that acts as the hole transport layer, with 1 nm SiO₂

as the buffer layer as shown in Fig. 1. We deposit modified Langmuir–Schaefer films (two to three monolayer's) of CdSe:ZnS (Evident Technologies) core-shell colloidal QDs via microcontact printing (μ CP) [Figs. 1(a) and 1(b)] using polydimethylsiloxane (PDMS) stamp, as we developed previously.²⁶ QDs sizes are typically varied and obtained by controlled precipitation process.²⁵ The electron transport layer is a mixture of cosputtered ZnO and SnO₂ [Fig. 1(c)]. The structure is completed by e-beam evaporating 15 nm thick aluminum (Al) cathode onto ZnO:SnO₂ layer. Optical transparencies of the ZnO:SnO₂ films for visible wavelengths were measured to be 90%. Fabricated diodes were then postprocessed using conventional lithographic techniques. Standard fabrication tools are used without any modifications. AZ5209A photoresist was spin coated and exposed [Figs. 1(d) and 1(e)]. Patterns with feature size 5 μ m were developed using AZ726MIF then baked at 90 °C. The pattern was etched into the device using reactive ion etching (RIE) technique with a gas mixture of CF₄ and Cl₂ to etch the Al layer. Longer etching time etched ZnO:SnO₂ and QD layer as shown in Fig. 1(f). Residual resist was removed by using alcohol and plasma cleaning.

The light emitting area can be defined either by patterning the QD layer or the cathode. A combined patterning technique where the top electrode is patterned over patterned QDs was used to form a QD-LED. Figure 2(a) shows electroluminescence of the diode at 4 V. Arrayed pattern of monolayer's of CdSe:ZnS particles of size 9.0 nm were stamped onto Si substrate. The Al cathode was then patterned

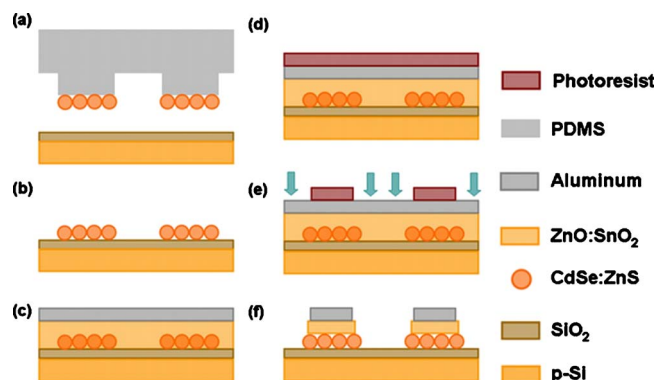


FIG. 1. (Color online) Fabrication process of QD-LED.

^{a)} Author to whom correspondence should be addressed. Electronic mail: john.zhang@engr.utexas.edu. Tel.: (512) 475-6872. FAX: (512) 232-4275.

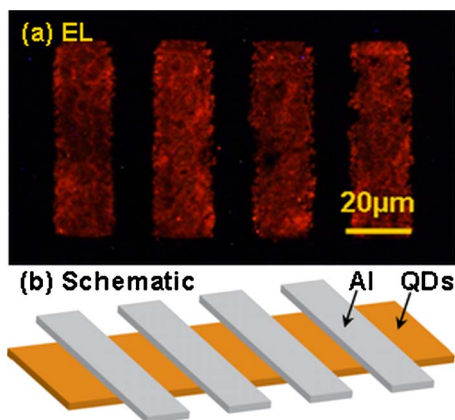


FIG. 2. (Color online) (a) EL observed for patterned top electrodes with feature size $20\ \mu\text{m}$; (b) Schematic of patterned nanoparticles and Al electrode.

to form $20\ \mu\text{m}$ wide lines perpendicular to the QD pattern. Figure 2(b) gives a schematic of the device.

LEDs with different QD particle diameters, namely 9.8 nm, 9.0 nm, 8.4 nm, and 7.8 nm, for emission wavelength 620 nm, 600 nm, 580 nm, and 560 nm, respectively, were tested with the same device configuration. Figure 3 gives the photoluminescence (PL) and electroluminescence (EL) spectra for 600 and 560 nm LEDs. The EL spectra measured are well correlated with the PL (full width half maximum of ~ 40 nm). An increase in EL intensity was observed with increased current injection. Figure 4(a) shows the current density versus voltage and EL intensity characteristics. The luminance of the devices for emission wavelength 620, 600, 580, and 560 nm was measured at 10 V and calculated to be 332, 487, 135, and 155 cd/m^2 . The measured emission area was $100 \times 100\ \mu\text{m}^2$. Current density of 12.3, 10.9, 12.0, and 19.9 mA/mm^2 and turn on voltage of 3.5 V, 4.0 V, 4.5 V, and 5.5 V with $1 \times 2\ \text{mm}^2$ top electrode was measured for 620 nm, 600 nm, 580 nm, and 560 nm diodes, respectively. Most diodes demonstrated steady light emission for over five hours of operation with Al as the cathode, proving the great stability of multi-layer structure [Fig. 4(b)]. Decrease in light emission was observed for diodes having Ag/Au as the cathode fabricated previously.²⁶ Use of Al as the top electrode enables better CMOS compatibility and postprocessing capability.

It is important to control patterning of both the light emitting layer and the metal cathode. We studied the limita-

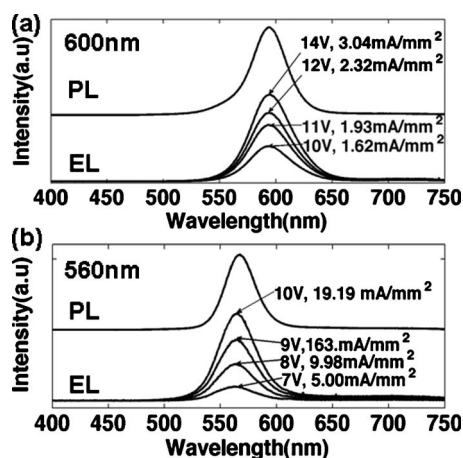


FIG. 3. EL and PL observed from particle size of (a) 9.0 nm, and (b) 7.8 nm.

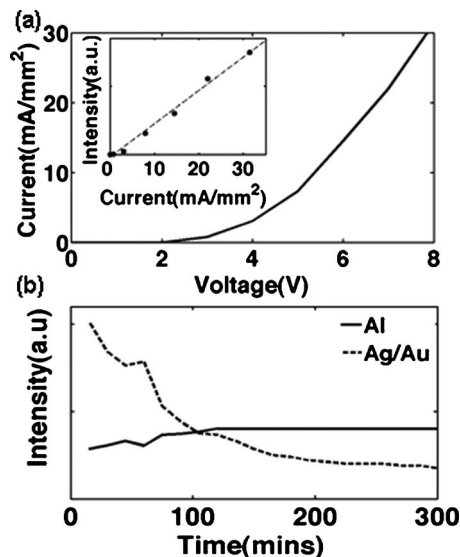


FIG. 4. (a) Current density vs voltage characteristics of a $2\ \text{mm}^2$ area QD-LED. Inset: EL intensity variation with current through the device. (b) Variation of EL intensity vs time with different cathode. (Emission wavelength of the diode 600 nm).

tion of two methods, namely (a) Nanopattern stamping which defines the area of patterned QDs and (b) Lithographic patterning of the top metal cathode that defines the area of charge injection. PDMS nanopattern stamps were used to transfer QDs onto the substrate. Nanoscale EL from QD-LEDs was observed (Fig. 5). Variation in light intensity of the pattern was due to nonuniformity in thickness of QDs deposited. As discussed previously, thicker QDs require more injection current, since they are highly resistive.²⁶ AFM was performed on the nanopatterned LED after observing EL from the device. Scanned feature size varied from 500×500 to $800 \times 800\ \text{nm}^2$. Variation in the size of patterned QD islands was due to the difficulty of creating a perfect PDMS replication of the nanopatterns, while the thickness distribution is attributed to our modified Langmuir-Schaefer film formation process. Height observed using AFM (~ 20 nm) was correlated with the EL intensity measured for the exact same region (Fig. 6) for particles with emission wavelength 600 and 560 nm. Microscope acts as a diffraction limited optical system. Resolving power of the objective is expressed as the point-spread function (PSF). Measured optical intensity is the convolution of the actual emitting area and the PSF. These intensity profiles were compared with the airy pattern that was theoretically calculated for our micro-

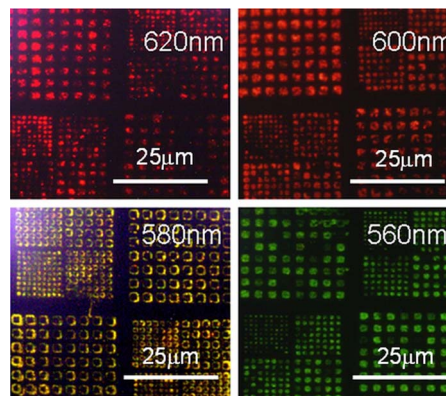


FIG. 5. (Color online) EL observed for different emission wavelength.

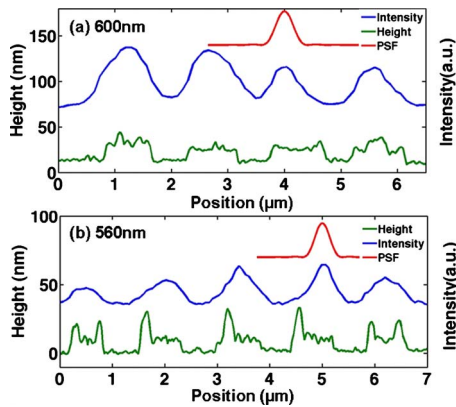


FIG. 6. (Color online) AFM vs EL for nanopatterned LEDs observed from particle size of (a) 9.0 nm (b) 7.8 nm.

scope objective [100 \times Olympus MPlan N, numerical aperture (NA) 0.9] and the emission wavelengths. The NA is among the highest available with an air medium. For certain cases, the emission profile was comparably as small as the PSF calculated (Fig. 6) indicating that smaller numbers of particles were electrically excited compared to the area of particles deposited. The emission profile is mainly defined by the PSF of the microscope. The actual emitting areas are estimated to be smaller than 100 nm. In other cases the EL intensity peak profile was larger than the AFM measured profile, indicating that the entire 500 \times 500 nm² area of particles were electrically excited. The EL profiles for those cases are still largely affected by the PSF.

For lithographically patterned LEDs, the smallest feature size of the electrode was 5 μ m (Fig. 7). A large area (4 mm²) of QDs was stamped and subsequent layers were deposited. The diodes were postprocessed and no significant damage was observed, proving that our device is robust for standard device fabrication processes. On application of voltage (\sim 3.5 V), light emission (wavelength 600 nm) was observed from the patterned top Al electrode. AFM measurement was performed on patterned electrode and correlated with the EL intensity. Double-lined edges can be found on the sides of each line in the AFM image [Fig. 7(c)]. This indicates two steps in the AFM profile of an edge (Fig. 7). The EL measurement corresponds to the inside 5 μ m wide

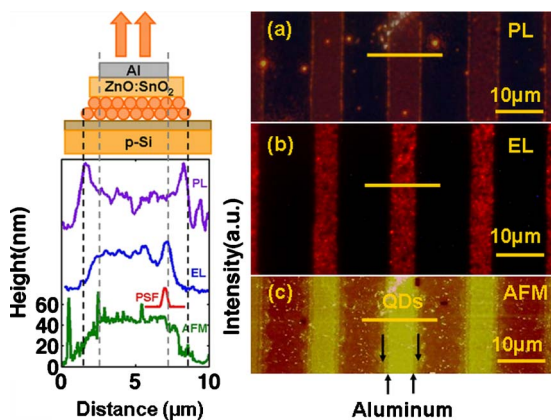


FIG. 7. (Color online) (Left) Schematic of patterned Al electrode and measured values of PL, EL and AFM at the horizontal lines indicated in the images on the right (Right) Patterned metal cathode (a) PL (b) EL and (c) AFM of etched Al electrode with 5 μ m feature size. Arrows in the bottom indicate Al step and the arrows on top indicate the QD step.

stripe pattern [Fig. 7(b)], and the PL measurement to the outside 8 μ m wide pattern [Fig. 7(a)]. This suggests that the inside stripes are Al layer and the outside pattern QD layer. The QD layer had a height of \sim 25 nm and the total layers had a height of 45 nm. The increasing and decreasing profile edge of the EL is similar to that of the PSF of the microscope. This indicates that the actual emitting area is comparable to the step function defined only by the geometry of patterned Al.

In summary, we demonstrated lithographical patterning of metal cathode of top emitting QD-LEDs on Si. The feature size of 5 μ m was achieved. The ease of fabrication and post processing open up possibilities for nanophotonic systems integrated with silicon electronics.

We thank NSF CAREER under Program No. ECCS-0846313 and NSF EPDT under Program No. ECCS-0725886 for financial support.

- ¹H. X. Jiang, S. X. Jin, J. Li, J. Shakya, and J. Y. Lin, *Appl. Phys. Lett.* **78**, 1303 (2001).
- ²T. Dobbertin, E. Becker, T. Benstem, G. Ginev, D. Heithecker, H. H. Johannes, D. Metzendorf, H. Neuner, R. Parashkov, and W. Kowalsky, *Thin Solid Films* **442**, 132 (2003).
- ³G. Gu and S. R. Forrest, *IEEE J. Sel. Top. Quantum Electron.* **4**, 83 (1998).
- ⁴K. Hoshino, L. J. Rozanski, D. A. V. Bout, and X. Zhang, *Appl. Phys. Lett.* **92**, 131106 (2008).
- ⁵E. Menard, M. A. Meitl, Y. Sun, J. U. Park, D. J. L. Shir, Y. S. Nam, S. Jeon, and J. A. Rogers, *Chem. Rev.* **107**, 1117 (2007).
- ⁶B. Kuswandi, J. Huskens, and W. Verboom, *Anal. Chim. Acta* **601**, 141 (2007).
- ⁷C. D. Müller, A. Falcou, N. Reckefuss, M. Rojahn, V. Wiederhirn, P. Rudati, H. Frohne, O. Nuyken, H. Becker, and K. Meerholz, *Nature (London)* **421**, 829 (2003).
- ⁸F. Papadimitrakopoulos, X. M. Zhang, D. L. Thomsen, and K. A. Higginson, *Chem. Mater.* **8**, 1363 (1996).
- ⁹D. G. Lidzey, M. A. Pate, M. S. Weaver, T. A. Fisher, and D. D. C. Bradley, *Synth. Met.* **82**, 141 (1996).
- ¹⁰C. C. Wu, J. C. Sturm, R. A. Register, and M. E. Thompson, *Appl. Phys. Lett.* **69**, 3117 (1996).
- ¹¹P. F. Tian, P. E. Burrows, and S. R. Forrest, *Appl. Phys. Lett.* **71**, 3197 (1997).
- ¹²H. Yamamoto, J. Wilkinson, J. P. Long, K. Bussman, J. A. Christodoulides, and Z. H. Kafafi, *Nano Lett.* **5**, 2485 (2005).
- ¹³L. Kim, P. O. Anikeeva, S. A. Coe-Sullivan, J. S. Steckel, M. G. Bawendi, and V. Bulovic, *Nano Lett.* **8**, 4513 (2008).
- ¹⁴P. F. Tian, V. Bulovic, P. E. Burrows, G. Gu, S. R. Forrest, and T. X. Zhou, *J. Vac. Sci. Technol. A* **17**, 2975 (1999).
- ¹⁵Z. H. Huang, G. J. Qi, X. T. Zeng, and W. M. Su, *Thin Solid Films* **503**, 246 (2006).
- ¹⁶S. Noach, E. Z. Faraggi, G. Cohen, Y. Avny, R. Neumann, D. Davidov, and A. Lewis, *Appl. Phys. Lett.* **69**, 3650 (1996).
- ¹⁷C. Kim, P. E. Burrows, and S. R. Forrest, *Science* **288**, 831 (2000).
- ¹⁸K. Hoshino, T. Hasegawa, K. Matsumoto, and I. Shimoyama, *Sens. Actuators, A* **128**, 339 (2006).
- ¹⁹J. Yu and V. Bulovi, *Appl. Phys. Lett.* **91**, 043102 (2007).
- ²⁰D. A. Pardo, G. E. Jabbour, and N. Peyghambarian, *Adv. Mater.* **12**, 1249 (2000).
- ²¹J. Bharathan and Y. Yang, *Appl. Phys. Lett.* **72**, 2660 (1998).
- ²²T. Granlund, T. Nyberg, L. S. Roman, M. Svensson, and O. Inganäs, *Adv. Mater.* **12**, 269 (2000).
- ²³W. S. Beh, K. In Tae, Q. Dong, X. Younan, and M. W. George, *Adv. Mater.* **11**, 1038 (1999).
- ²⁴K. Y. Suh, Y. S. Kim, and H. H. Lee, *Adv. Mater.* **13**, 1386 (2001).
- ²⁵B. O. Dabbousi, J. Rodriguez-Viejo, F. V. Mikulec, J. R. Heine, H. Mattoussi, R. Ober, K. F. Jensen, and M. G. Bawendi, *J. Phys. Chem. B* **101**, 9463 (1997).
- ²⁶A. Gopal, K. Hoshino, S. Kim, and X. Zhang, *Nanotechnology* **20**, 235201 (2009).